POLITECNICO DI TORINO
Repository ISTITUZIONALE

A Simulation Environment for Directional Sensing as a Phase Separation Process

(Article begins on next page)

A Simulation Environment for Directional Sensing as a Phase Separation Process

Antonio de Candia,[1] Andrea Gamba,[2]* Fausto Cavalli,[3] Antonio Coniglio,[1]
Stefano Di Talia,[4] Federico Bussolino,[5] Guido Serini[5]*

[1]Department of Physical Sciences, Università di Napoli "Federico II," Istituto Nazionale di Fisica della Materia, and Istituto Nazionale di Fisica Nucleare, Unità di Napoli, 80126 Napoli, Italy. [2]Department of Mathematics, Politecnico di Torino, Corso Duca degli Abruzzi 24, 10129 Torino, and Istituto Nazionale di Fisica Nucleare, Unità di Torino, Via Giuria 1, 10125 Torino, Italy. [3]Department of Mathematics, Università degli Studi di Milano, Via Saldini 50, 20133 Milano, Italy. [4]Laboratory of Mathematical Physics, The Rockefeller University, 1230 York Avenue, New York, NY 10021, USA. [5]Department of Oncological Sciences and Division of Molecular Angiogenesis, IRCC, Institute for Cancer Research and Treatment, University of Torino School of Medicine, Strada Provinciale 142 Km 3.95, 10060 Candiolo (TO), Italy.

*Corresponding authors. E-mail: andrea.gamba@polito.it (A.G.); guido.serini@ircc.it (G.S.)

Abstract

The ability of eukaryotic cells to navigate along spatial gradients of extracellular guidance cues is crucial for embryonic development, tissue regeneration, and cancer progression. One proposed model for chemotaxis is a phosphoinositide-based phase separation process, which takes place at the plasma membrane upon chemoattractant stimulation and triggers directional motility of eukaryotic cells. Here, we make available virtual-cell software that allows the execution and spatiotemporal analysis of in silico chemotaxis experiments, in which the user can control physical and chemical parameters as well as the number and position of chemoattractant sources.

Introduction

Guided cell motility is crucial for the development of multicellular organisms (*1*), for example, during the assembly of the cardiovascular (*2*), nervous (*3*), and musculoskeletal (*4*) systems. Moreover, in the adult organism, directed cell movement plays a major role in physiological and pathological settings such as wound healing, angiogenesis, immune response, and cancer (*5*). Therefore, there is interest in dissecting the molecular dynamics by which gradients of chemoattractants stimulate directed cell motion—that is, chemotaxis.

In several cell types, a shallow chemoattractant gradient gives rise to an unamplified receptor activation gradient. The activated receptors in turn elicit the recruitment of phosphatidylinositol 3-kinase (PI3K) from the cytosol to the plasma membrane, where it greatly amplifies chemotactic signaling by converting phosphatidylinositol 4,5-bisphosphate (PIP_2) into phosphatidylinositol 3,4,5-trisphosphate (PIP_3) and giving rise to sharply segregated PIP_2- and PIP_3-rich phases (*1*). The phosphatase PTEN counterbalances the enzymatic activity of PI3K by dephosphorylating PIP_3 into PIP_2. Docking of cytosolic PTEN at the cell membrane depends on the short N-terminal PIP_2-binding domain (PBD) and is required for its activity (*6*, *7*). As a result, PI3K and PIP_3 accumulate on the plasma membrane at the side facing the highest chemoattractant concentration, whereas PTEN and PIP_2 display a complementary distribution (*1*). Such an early symmetry-breaking event constitutes the first fundamental step of chemotaxis and is usually defined as directional sensing (*8*). Afterward, a cell polarization phase follows, during which binding of pleckstrin homology (PH) domain–containing effector proteins to PIP_3 triggers polarized cytoskeletal and adhesive dynamics that finally translate into directed cell motion (*9*). Hence, directional sensing lies upstream of cell polarization, from which it can be functionally decoupled by treating cells with actin polymerization inhibitors (*10*). Notably, chemoattractants stimulate the formation of self-organizing small PIP_3 patches, which drive localized actin polymerization and cell protrusion (*11*–*13*).

A physical and computational modeling approach can prove useful in testing and unveiling the identity of minimal biochemical networks whose dynamics can incorporate the blueprints for complex cellular functions, such as chemotaxis. Previous models (*8*, *14*–*16*) based on a local activator and a global inhibitor did not satisfactorily reconcile several key aspects of directional sensing, such as insensitivity to absolute stimulation values, large amplification of shallow chemoattractant gradients, reversibility of phase separation, robustness with respect to parameter perturbations, the stochastic character of cell responses, and the use of realistic biochemical parameters and space-time scales.

However, all of these aspects follow naturally from the observation that the network of chemical reactions, which constitutes the backbone of directional sensing, presents a physical instability toward spontaneous phase separation (*17*). In this framework, directional sensing appears as the result of a nucleation process by which a spot rich in PIP_2 and PTEN is created in a sea rich in PIP_3 and PI3K. Slight anisotropies (i.e., variations in the concentrations in a particular direction) in the extracellular chemoattractant landscape drive and accelerate the process of spot formation, taking advantage of the underlying phase separation instability. This way, the reaction-diffusion dynamics taking place on the two-dimensional cell membrane works as a powerful amplifier of shallow gradients in the distribution of the external chemical signal.

To allow easy experimentation of the phase separation paradigm and its comparison with other models of directional sensing (*8*, *14*–*16*), we provide an easy-to-use simulation environment, called DirSens, where physical and chemical parameters can be set and the surface distribution of the relevant chemical factors can be observed in real time. The underlying kinetic code simulates the stochastic chemical evolution on a spherical surface (representing the cell plasma membrane) coupled to an enzymatic reservoir (representing the cytosol).

Equipment

Personal computer equipped with the Windows or Linux operating system

Java plug-in, Java Runtime Environment (www.java.com/en/download/index.jsp)

DirSens simulation environment software (Windows: approximately 1.2 MB download, 6 MB uncompressed; Linux: approximately 1.2 MB download, 5.3 MB uncompressed) (http://stke.sciencemag.org/cgi/content/full/sigtrans;2007/378/pl1/DC1)

Instructions

These instructions include explicit commands or computer filenames. They are set off by quotation marks. Do not type the quotation marks when typing the commands.

Various biochemical parameters and kinetic parameters can be set (Table 1). The physical and chemical parameters for the simulation are assigned using the input boxes, and the default settings may be changed by either typing a new value into the input box or using the up and down arrow buttons (Fig. 1A). Most parameters are common biochemical or kinetic parameters, except the seed for random number generation (Seed), which is an integer number required to initialize the stochastic algorithm. A positive integer value for Seed gives rise to a random but exactly reproducible evolution of the system in time. All positive integer values of Seed are statistically equivalent. This means, for instance, that if biochemical and kinetic parameters are such as to produce random polarization, all positive integer values of Seed will produce random polarization, but the actual direction of polarization will differ from one value of Seed to another. The user can change the value of Seed to check the robustness of the obtained results—that is, the independence of the results on the particular sequence of random numbers produced by the algorithm. When Seed is set to zero, the system undergoes an unpredictable random evolution, which is different for each simulation session.

The distribution of activated receptors is described by two parameters: (i) a spatially uniform background concentration of receptors Crec, and (ii) a gradient with an amplitude controlled by the parameter Veps. The constant component Crec may be defined by the user at the beginning but cannot be modified during the course of the simulation. Instead, the percent anisotropy Veps can be modified in real time. Alternatively, the two-component description controlled by Crec and Veps can be replaced with a user-defined activation landscape produced by localized external sources (Fig. 1B).

By default, the visualization output (graphs and images) includes the changes in PIP_2 ([PIP2] field) and PIP_3 ([PIP3] field) concentrations, as well as the order parameter g, which indicates the degree of symmetry breaking in the spatial distribution of the PIP_2-to-PIP_3 concentration difference (*17*). The Visualization Options button (Fig. 1C) allows the user to select additional data to be displayed. The options and their values are described in Table 2. The user can specify the order of the output in columns and rows that will appear in the System State window by choosing to add (or remove) rows or columns (limit is 5 for both) from the Visualization Options window (Fig. 2). Rows are removed from the bottom and columns are removed from the right. To return to the default visualization settings, the program must be closed and restarted. While the simulation is running and after it is complete, the data will appear in a window called System State (Fig. 3). A window called Visualization Control will allow the user to pan through a completed simulation (Fig. 3, inset). The three-dimensional representations of the cell in the System State window can be rotated to view different sides of the cell by dragging them with the mouse.

Once the parameters are defined, the simulation is started by clicking the Start Simulation button and can be stopped before time Tmax by clicking the Stop Simulation button. The Visualization Control window shows the elapsed time of the simulation (Fig. 3). After the simulation is complete, the buttons on the Visualization Control window can be used to pan the simulation forward or backward in time. If the pause button (‖) is clicked during the simulation, the simulation must be restarted from time zero using the DirSens Control window. The < and > arrowheads step the simulation backward or forward incrementally, based on the user-defined time step; the << and >> arrowheads replay the simulation backward or forward; and the <<< and >>> arrowheads set the simulation at the end (Tmax) or the beginning. The slider allows the user to pan smoothly forward and backward in time. The color scale default is "Single time" for the cell representations, which allows the scale to change during the simulation to provide optimized visualization of differences in the concentrations of the various elements at any given time. This can be changed to a static color scale that represents the concentration ranges during the entire simulation ("All times"); however, the differences in concentrations at any given time will be more difficult to visualize using this setting.

Most physical and kinetic parameters can be modified in real time while a simulation is running by changing them in the input boxes and clicking the Refresh Parameters button, thus allowing the user to test the effect of abrupt changes of the environmental conditions. The input boxes for those parameters that cannot be modified in real time are disabled. The "Set pars as default" button allows saving the present set of parameters to be saved in such a way that the software will use these settings automatically the next time the program is run.

Simulations can be saved as "sessions." The files are saved into the folder called "session" in the "Dirsens_win" directory and are named by date and time; for example, a session saved on 8 January 2007 at 12:50 PM is named "sess_200701081250." Files may be copied, but cannot be moved, or the software will not be able to retrieve a saved session.

The raw data obtained by the simulation are stored in the folder called "tmp" when the program is running and in the "session" folder when a session has been saved. They can be easily extracted and processed with standard programs for scientific visualization. The parameters used in the simulation are listed in the "pars" and "pars_xx" files. The rows of the "hist" file contain the average concentrations of chemical factors at subsequent times. The rows of the "state_xxxxx" files contain concentrations of chemical factors at time xxxxx in sequentially ordered sites of the lattice. The space coordinates of each lattice site are specified in the first three columns of the "hex.nn+10242" file contained in the "data" folder. Sites are listed in the same order in the "state_xxxxx" files and in the "hex.nn+10242" file. For a detailed description of the content of the "hist" and "state_xxxxx" files, see Tables 3 and 4.
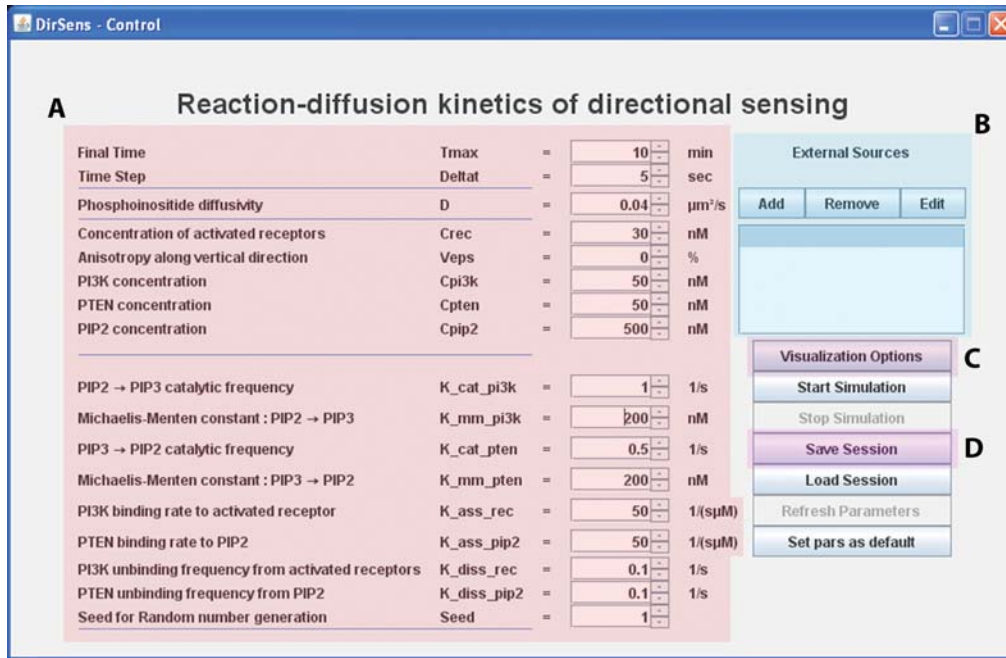
Fig. 1. The main control panel of the DirSens Simulation Environment. (**A**) Kinetic and physical constants are adjustable. (**B**) Coordinates and intensities of one or more localized chemoattractant sources can be set. (**C**) The user can specify the visualization in real time of different quantities, such as local or global concentration of chemical factors. (**D**) Simulation sessions can be saved and recalled for future analysis.

Parameter	Definition	Units	Default settings
T max	Total simulated time	Minutes	30
Deltat	Simulated time between two successive visualizations	Seconds	5
D	Phosphoinositide diffusivity, which is the diffusion coefficient of PIP_2 and PIP_3 in the membrane	$\mu m^2/s$	1
Crec	Concentration of activated receptors	NanoMolar	50
Veps	Anisotropy along the vertical direction, which is the change in chemoattractant concentration in the vertical direction	Percent change	0
Cpi3k	Concentration of PI3K	NanoMolar	50
Cpten	Concentration of PTEN	NanoMolar	50
Cpip2	Concentration of PIP_2	NanoMolar	500
K_cat_pi3k	Rate constant for the conversion of $PIP_2 \longrightarrow PIP_3$	$Seconds^{-1}$	1
K_mm_pi3k	Michaelis-Menten constant for PI3K	NanoMolar	200
K_cat_pten	Rate constant for the conversion of $PIP_3 \longrightarrow PIP_2$	$Seconds^{-1}$	0.5
K_mm_pten	Michaelis-Menten constant for PTEN	NanoMolar	200
K_ass_rec	Rate at which PI3K binds to the activated receptor (Crec)	$(seconds \cdot \mu M)^{-1}$	50
K_ass_pip2	Rate at which PTEN binds to PIP_2	$(seconds \cdot \mu M)^{-1}$	50
K_diss_rec	Frequency at which PI3K dissociates from the activated receptors	$Seconds^{-1}$	0.1
K_diss_pip2	Frequency at which PTEN dissociates from PIP_2	$Seconds^{-1}$	0.1
Seed	Random number generation	Positive integer or zero	1

Table 1. Biochemical and kinetic parameters that can be specified by the user in DirSens. Default settings are within in the physiological range.
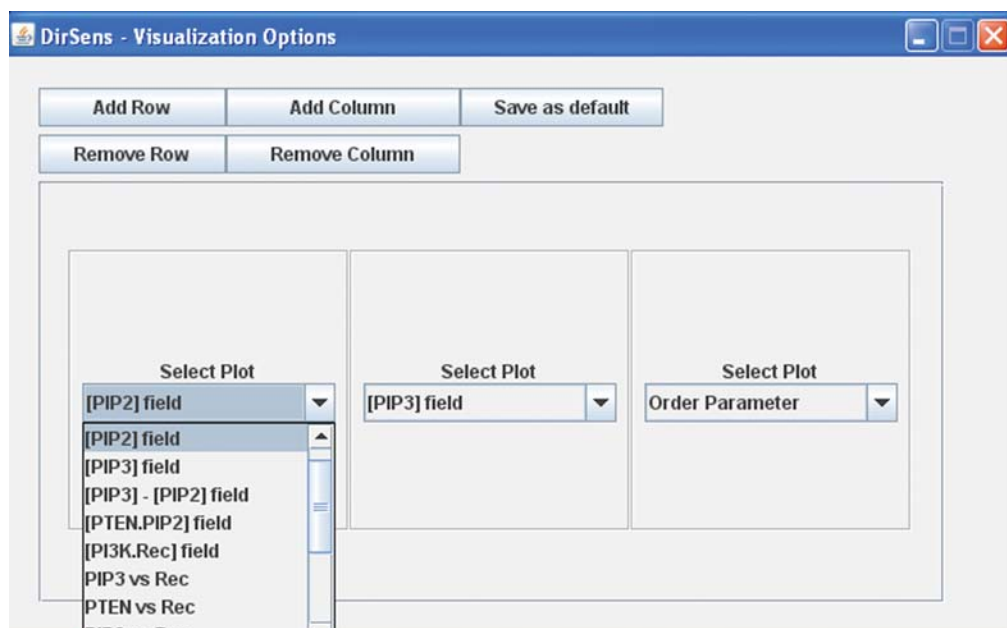
Fig. 2. The Visualization Options window. This window allows the user to choose what data will display with the simulation. Up to five rows and columns may be added and any of the 14 possible data outputs can be placed in any position. Data output options are selected from a drop-down menu.

Selection	Output	Explanation
[PIP2] field	3-D cell image	The concentration of PIP_2 on the surface at any time in the simulation.
[PIP3] field	3-D cell image	The concentration of PIP_3 on the surface at any time in the simulation.
[PIP3]-[PIP2] field	3-D cell image	The differences in the concentrations of PIP_3 and PIP_2 on the surface at any time in the simulation.
[PTEN.PIP2] field	3-D cell image	The concentration of PTEN bound to PIP_2 on the surface at any time in the simulation.
[PI3K.Rec] field	3-D cell image	The concentration of PI3K bound to activated receptor on the surface at any time in the simulation.
PIP3 vs Rec	Graph	Concentration of PIP_3 (y-axis) versus the concentration of activated receptors (x-axis)*. The dotted line is an interpolation of the experimental points and the solid line is the diagonal of the axes.
PTEN vs Rec	Graph	Concentration of PTEN (y-axis) versus the concentration of activated receptors (x-axis)*. The dotted line is an interpolation of the experimental points and the solid line is the diagonal of the axes.
PIP2 vs Rec	Graph	Concentration of PIP_2 (y-axis) versus the concentration of activated receptors (x-axis)*. The dotted line is an interpolation of the experimental points and the solid line is the diagonal of the axes.
PIP2 average vs time	Graph	PIP_2 average concentration (y-axis) over time (x-axis).
PIP3 average vs time	Graph	PIP_3 average concentration (y-axis) over time (x-axis).
PTEN.PIP2. aver. vs time	Graph	Average concentration of PTEN bound to PIP_2 on the surface (y-axis) over time (x-axis).
PI3K.Rec aver. vs time	Graph	Average concentration of PI3K bound to activated receptor on the surface (y-axis) over time (x-axis).
Harmonic components	Graph	Relative weight of the first 6 harmonic components (y-axis)* over time (x-axis).
Order Parameter	Graph	The degree of symmetry breaking in the spatial distribution of the PIP_2 to PIP_3 concentration difference (y-axis) over time (x-axis).

Table 2. Visualization options. *Refer to (*17*) for details of the calculations.
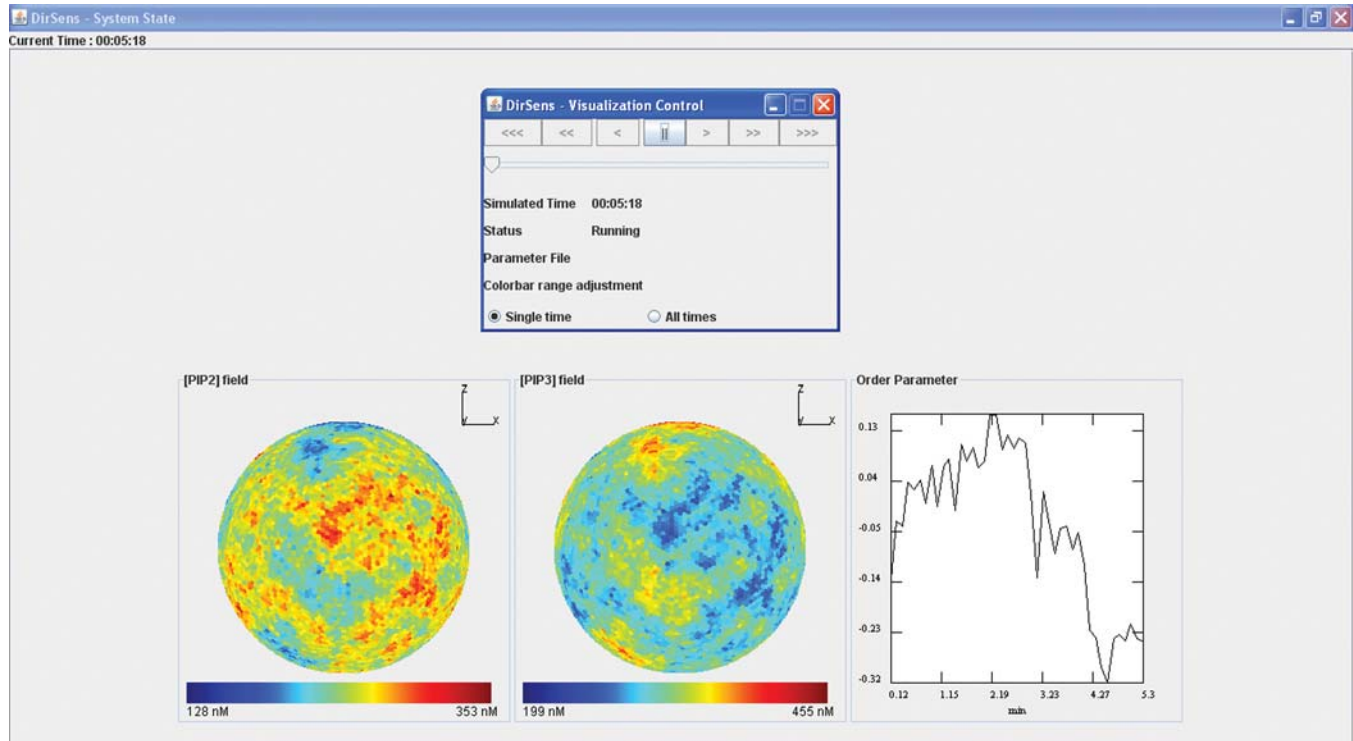
Fig. 3. The System State window and Visualization Control panel from a 10-min simulation captured ~6 min into the simulation. The Visualization Control panel partially covers the System State window. The data selected to be output appears in the System State window; in this case, there is one row of data with three columns. The cell representations can be rotated in three-dimensional space by dragging them with the mouse. Each cell representation will set to the new orientation. Once the simulation is complete, the user can move forward or backward in time through the data by using the buttons at the top of the Visualization Control panel or using the slider. The colorbar range adjustment allows the user to specify whether the color scale for the cell representations should change during the simulation ("Single time") or should be constant throughout the simulation ("All times").

Column number	1	2	3	4	5	6	7	8	9	10	11	12	13	14	15-25
Column content	Iteration number	Percent free PI3K	Percent bound PI3K	*	Percent free PTEN	Percent bound PTEN	Average number of PIP_3 molecules per lattice site	*	Average number of PIP_2 molecules per lattice site	*	*	*	*	Binder cumulant	*

Table 3. Order of appearance of data in the columns of the "hist" file. *For internal use by the software.

Column number	1	2	3	4	5	6
Column content	Number of activated receptors	Number of PIP_2 molecules	Number of PIP_3 molecules	Number PTEN molecules	*	Number of PI3K molecules

Table 4. Order of appearance of data in the columns of the "state_xxxxx" file. The nth row of the "state_xxxxx" file contains the number of molecules on site n at time xxxxx. The space coordinates of site n are given in the first three columns of the nth row of the "hex.nn+.10242" file contained in the "data" folder. *For internal use by the software.

To illustrate the use of the simulation environment, we describe several sample "experiments." Users are encouraged to consider these as just a starting point and to try different values and combinations of the adjustable parameters. Installation instructions are provided for Windows and Linux. Because each session can be saved, the software must be downloaded and run from the user's computer.

Installation for Windows

1. Download the "Dirsens_win.zip" file.

2. Unzip in a directory of your choice.

3. Go to the "java" folder in the folder containing the unzipped files and double-click the file called "dirsens.jar" to launch the simulation.

Installation for Linux

1. Download the "Dirsens.tar.gz" file.

2. Unzip in a directory of your choice.

3. Open a terminal and run ". ./install".

4. Go to the directory "java" and type "java -jar dirsens.jar" to launch the simulation.

Insensitivity to Uniform Chemoattractant Stimulation

In this simulation, phase separation does not occur during the observation time. The phosphoinositide concentrations fluctuate in space over a uniform background, and no symmetry breaking is observed (Fig. 4A). Spots enriched in either PIP_2 or PIP_3 are transiently formed but rapidly decay. Accordingly, the order parameter g fluctuates around the zero value.

If this same simulation is performed but allowed to proceed for 100 min instead of 40, then spontaneous symmetry breaking can be observed. After about 45 min of simulated time, spontaneous symmetry breaking takes place with the formation of randomly oriented PIP_2- and PIP_3-rich clusters (Fig. 4B). The instructions for the 40-min simulation are provided, but the only difference is the Tmax setting to run the 100-min simulation.

Running and Saving a Simulation

1. Launch the simulation environment.

2. Set $D = 0.4\ \mu m^2/s$, Crec = 30 nM, Tmax = 40 min, Veps = 0.

3. Using the default visualization options, click the Start Simulation button. Allow it to run to completion.

> *Note: The DirSens-System State window and the DirSens-Visualization Control window will both open when the simulation is started. Depending on the size of the monitor, the windows may not all be visible at the same time. The DirSens Control window will also remain open. Windows may be minimized using the "-" button in the upper right. Windows that are required for the simulation cannot be closed with "x".*

4. From the System State window, view the graphs and three-dimensional representations of the cell based on the default visualization options.

5. From the Visualization Control window, monitor the status of the simulation; once it is complete, use the buttons to move forward and back in time through the data.

> *Note: If the pause button (||) on the Visualization Control window is clicked during the simulation, the simulation must be restarted from time zero using the DirSens Control window.*

6. From the Control window, click the Save Session button to save the data from this simulation.

> *Note: This is optional. The files will be saved in the session folder. If the simulation is not saved, the data are available as long as a new simulation is not started and DirSens remains open.*

7. Close the simulation environment by clicking the "x" at the top right of the Control window.

Rerunning a Saved Session and Changing the Visualization Options

1. Launch the simulation environment.

2. Load a simulation by clicking the "Load Session" button.

3. Choose the file from the window.

4. Use the Visualization Control panel to replay the simulation from the beginning to step through the simulation to view the data at any given point in time.

5. To change the Visualization Options, add rows or columns and select the data to display.

6. Click the "Save as default" button.

7. To view the additional data, load the saved simulation again from the Control panel by clicking the Load Session button. The software will now display the additional selected graphs or cell representations in the System State window.
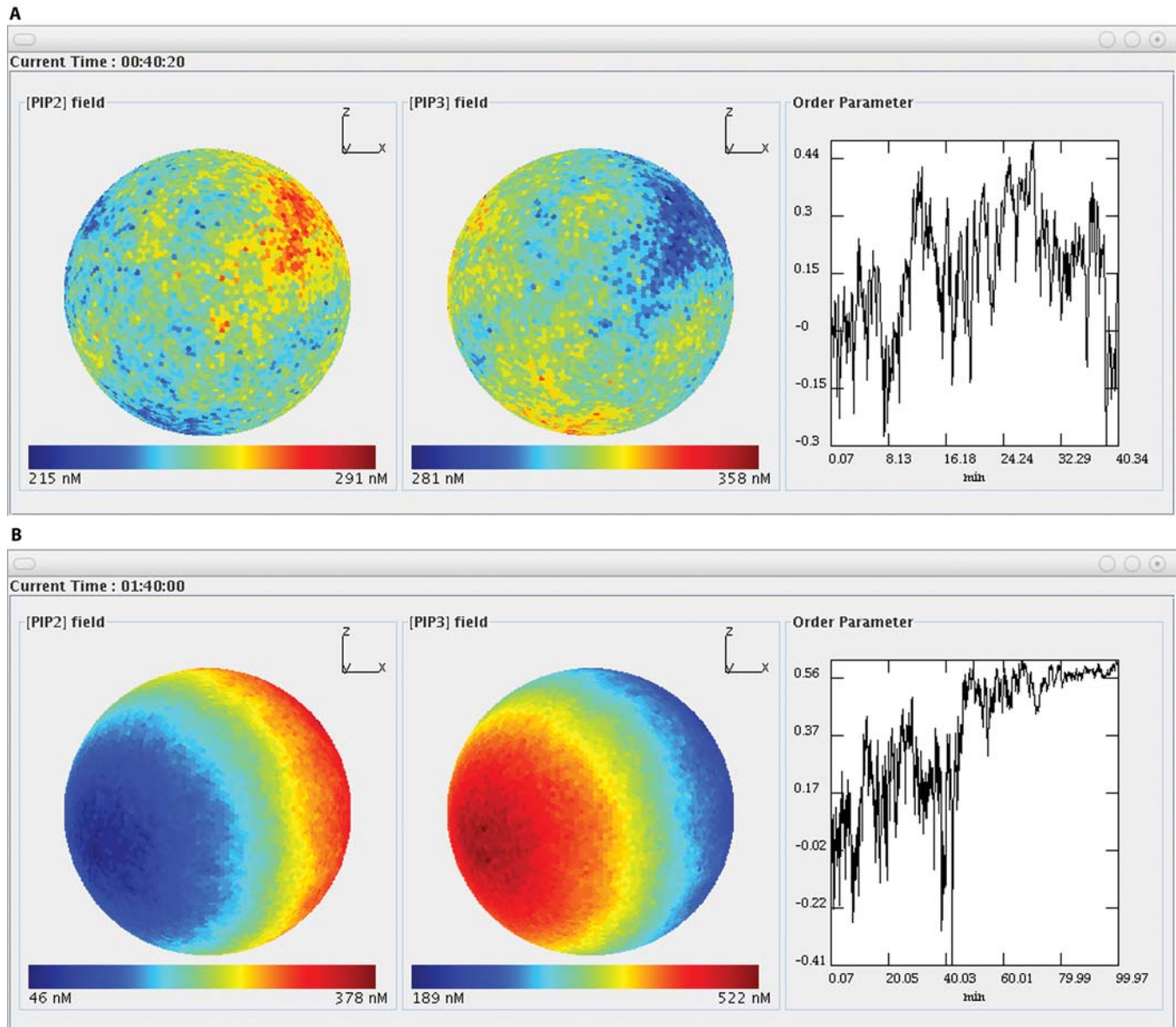
Fig. 4. (**A**) Simulation for 40 min under conditions of uniform stimulation. Left, surface PIP$_2$ distribution; center, PIP$_3$ distribution; right, order parameter, which gives a quantitative measure of the degree of spatial symmetry breaking in the phosphoinositide concentration. (**B**) Simulation for 100 min under conditions of uniform stimulation shows spontaneous symmetry breaking taking place around $t =$ 45 min. After the formation of separate PIP$_2$- and PIP$_3$-rich clusters (left), the order parameter (right) stabilizes around the value 0.6.

Symmetry Breaking Induced by Slightly Anisotropic Chemoattractant Stimulation

The initial steps are the same as those for the previous example of a uniform stimulation. However, after the simulation starts, the degree of stimulation is changed by changing the Veps value. The spatial symmetry in the phosphoinositide concentration is broken in a few minutes, and two complementary PIP$_2$- and PIP$_3$-rich clusters form along the anisotropy direction (Fig. 5).

1. Set D = 0.4 μm^2/s, Crec = 30 nM, Tmax = 40 min, Veps = 0.

2. Use the default visualization options, or choose the data to display using the Visualization Options button, and click the Start Simulation button.

3. After 10 min, from the Control window, change the Veps value to 5%.

4. Click the Refresh Parameters button.

Note: This change can be made at any time before the end of the simulation.

5. View the data in the System State window using the Visualization Control window to pan through the data once the simulation is complete.

6. From the Control window, save the simulation by clicking the Save Session button.
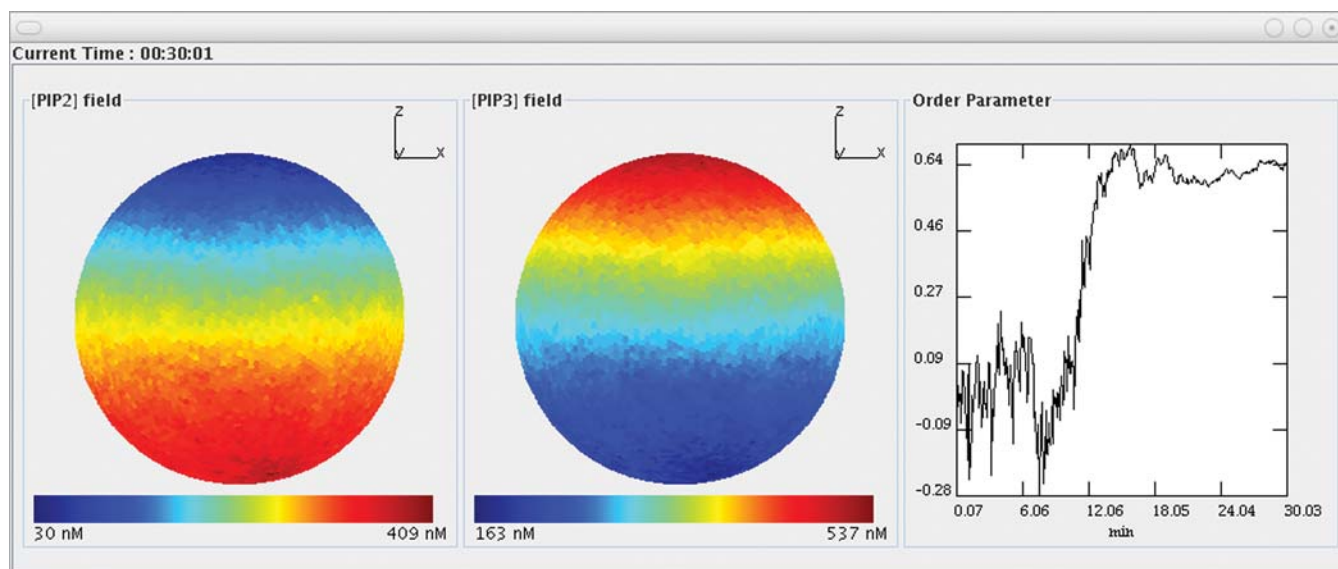
   Note: This is optional.

Fig. 5. Slightly anisotropic stimulation. After switching on a 5% anisotropic component in chemoattractant stimulation, two complementary PIP$_2$-rich (left) and PIP$_3$-rich (center) clusters form in a few minutes. The order parameter *g* (right) fluctuates close to the zero value until the anisotropic component is added; then it stabilizes around the value 0.6, signaling that symmetry breaking has occurred.

Defining Multiple Chemoattractant Sources

As many as three chemoattractant sources may be specified instead of using the Veps parameter to represent a vertical linear gradient. The format of the data for the user-defined chemoattractant sources is (i) coordinates of the source and (ii) rate of production in nM/s. The positions of the external sources (their spatial coordinates) with respect to the center of the cell and the rate of chemoattractant release are specified using the External Sources field in the Control window (Fig. 1B). The concentration for each chemoattractant source can be specified. In this simulation, two equal chemoattractant point sources are added in the X (horizontal) direction, one at +20 from the center and one at –20 from the center. Both have a rate of release of 10 nM/s. The simulation shows the formation of two opposed PIP$_3$-rich patches, each close to one of the two chemoattractant sources (Fig. 6).

1. Set D = 0.4 μm^2/s, Crec = 30 nM, Tmax = 40 min, and Veps = 0%.

   Note: The formation of the PIP$_3$-rich regions is apparent after only 5 min.

2. Click the Add button at the top of the External Sources box.

3. Type –20 in the space coordinate for X, 0 in the space coordinate for Y, 0 in the space coordinate for Z, and 10 in the value c for intensity, and click the Add button.

4. Click the Add button again at the top of the External Sources box.

5. Type 20 in the space coordinate for X, 0 in the space coordinate for Y, 0 in the space coordinate for Z, and 10 in the value c for intensity, and click the Add button.

6. Use the default visualization options, or choose the data to display using the Visualization Options button, and click the Start Simulation button.

7. To change or remove external sources, select the external source that you wish to change, and click the Edit or Remove button at the top of the External Sources box.

8. Click the Refresh Parameters button.

9. View the data in the System State window using the Visualization Control window to pan through the data once the simulation is complete.

10. From the Control window, save the simulation by clicking the Save Session button.
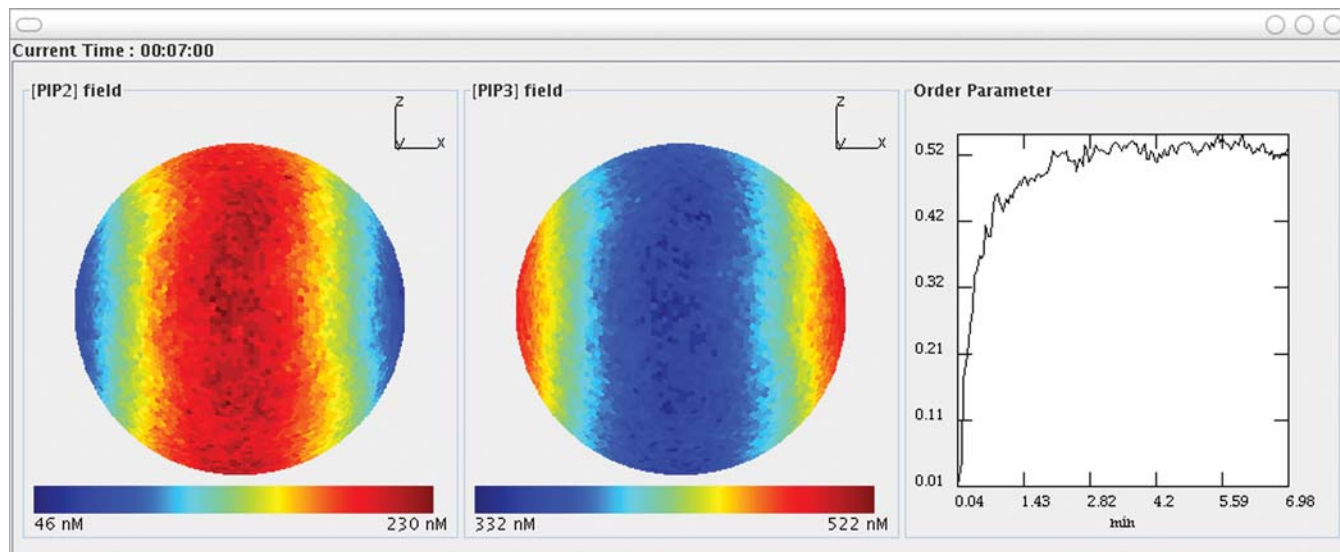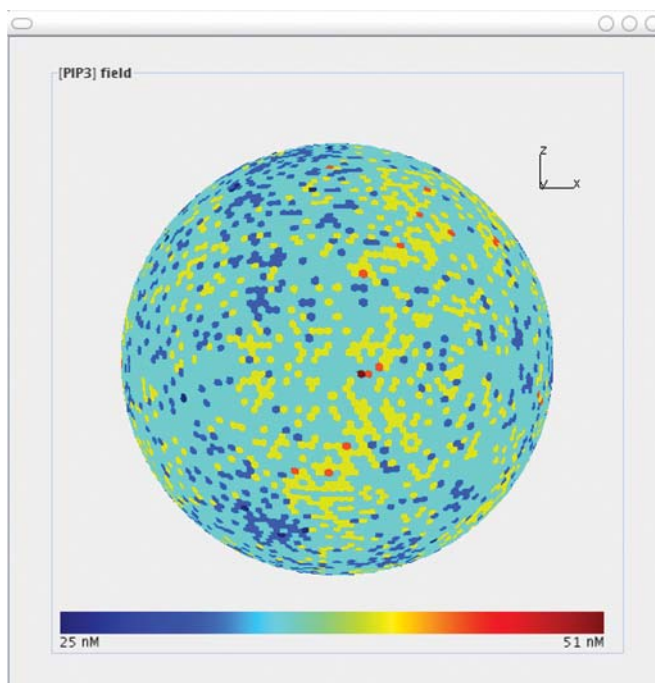
   Note: This is optional.

Fig. 6. Stimulation with multiple chemoattractant sources produces multiple PIP$_3$-rich patches. By adding two equal chemoattractant sources concentrated at coordinate points $x = -20$ and $x = 20$, one observes the formation of two opposed PIP$_3$-rich patches close to the two sources.

Formation of PIP$_3$ Patches Upon Uniform Stimulation with Low Chemoattractant Concentrations

When the concentration of activated receptors is too low, the PIP$_3$-rich patches are unable to assemble into larger clusters (Fig. 7). In this simulation, the concentration of activated receptors is decreased one order of magnitude from the default parameter values by setting Crec at 5 nM. Over time, the surface distribution of phosphoinositide concentrations shows the transient appearance of small PIP$_3$-rich patches all over the plasma membrane surface. Such patches rapidly form and disappear and are not able to assemble into clusters of larger size.

1. Set D = 0.4 μm^2/s, Crec = 30 nM, Tmax = 40 min, Veps = 0%, and Crec = 5 nM.

2. Use the default visualization options, or choose the data to display using the Visualization Options button, and click the Start Simulation button.

3. From the System State window, view the graphs and three-dimensional representations of the cell based on the default visualization options.

Fig. 7. Uniform stimulation with low activated receptor concentrations. Transient small PIP$_3$-rich patches are observed all over the plasma membrane surface.

4. View the data in the System State window using the Visualization Control window to pan through the data once the simulation is complete.

5. From the Control window, click the Save Session button to save the data from this simulation.

> *Note: This is optional. The files will be saved in the session folder. If the simulation is not saved, the data are available as long as a new simulation is not started and DirSens remains open.*

Troubleshooting

Users should always press the keyboard's Return or Enter key after inserting new parameter values in the input boxes, because with some Java versions they are otherwise not accepted. For a current simulation, parameter values can be checked by opening the "pars" file in the directory "tmp". This file can be opened with Notepad or a similar text editor and contains the values of each parameter (Table 5).

During the simulation, rare fluctuations occasionally produce sites with very low concentrations of the relevant factors. Because the ranges of the colorbar scales are adjusted automatically, this can lead to correspondingly large fluctuations in the graphed colors in time. This is a normal consequence of the visualization method adopted and should not be considered a problem. By selecting "Colorbar range adjustment—All times" in the Visualization Control window after the end of the simulation, a single colorbar range is used at all times.

Tmax	Deltat	Crec	Cpi3k	Cpten	Cpip2	Veps	D	K_cat _pi3k	K_cat _pten	K_mm _pi3k	K_mm _pten	*	K_ass _rec	K_ass _pip2	*	K_diss _rec	K_diss _pip2	*
10.0	5.0	30.0	50.0	50.0	500.0	5.0	0.4	1.0	0.5	200.0	200.0	0	50.0	50.0	0	0.1	0.1	0

Table 5. Sample values in the "pars" file from a 10-min simulation presented in the order in which they appear in the file. *Unused

Notes and Remarks

Stochastic modeling of reaction-diffusion systems takes into account the effects of random fluctuations in the constituent concentrations and in the rate of advancement of chemical reactions, whose relevance cannot be underestimated in a cellular environment. As shown by our model, they can be directly responsible for the high sensitivity of the system to small spatial anisotropies in the activation field, as well as for observed phenomena such as stochastic cell polarization.

For the implementation of the simulation environment, the public-domain package Jama (http://math.nist.gov/javanumerics/jama) has been used.

To ensure complete reproducibility of our results, we provide the simulation software and graphical user interface as open source, according to the General Public License (www.gnu.org/copyleft/gpl.html). They can be freely used and modified, as long as their use is acknowledged by citing this article and Gamba *et al*. (*17*).

References

1. P. J. Van Haastert, P. N. Devreotes, Chemotaxis: Signalling the way forward. *Nat. Rev. Mol. Cell Biol.* **5**, 626–634 (2004).
2. G. Serini, F. Bussolino, Common cues in vascular and axon guidance. *Physiology (Bethesda)* **19**, 348–354 (2004).
3. Z. Wen, J. Q. Zheng, Directional guidance of nerve growth cones. *Curr. Opin. Neurobiol.* **16**, 52–58 (2006).
4. F. Schnorrer, B. J. Dickson, Muscle building; mechanisms of myotube guidance and attachment site selection. *Dev. Cell* **7**, 9–20 (2004).
5. A. J. Ridley, M. A. Schwartz, K. Burridge, R. A. Firtel, M. H. Ginsberg, G. Borisy, J. T. Parsons, A. R. Horwitz, Cell migration: Integrating signals from front to back. *Science* **302**, 1704–1709 (2003).
6. M. Iijima, Y. E. Huang, H. R. Luo, F. Vazquez, P. N. Devreotes, Novel mechanism of PTEN regulation by its phosphatidylinositol 4,5-bisphosphate binding motif is critical for chemotaxis. *J. Biol. Chem.* **279**, 16606–16613 (2004).
7. F. Vazquez, S. Matsuoka, W. R. Sellers, T. Yanagida, M. Ueda, P. N. Devreotes, Tumor suppressor PTEN acts through dynamic interaction with the plasma membrane. *Proc. Natl. Acad. Sci. U.S.A.* **103**, 3633–3638 (2006).
8. P. Devreotes, C. Janetopoulos, Eukaryotic chemotaxis: Distinctions between directional sensing and polarization. *J. Biol. Chem.* **278**, 20445–20448 (2003).
9. M. Affolter, C. J. Weijer, Signaling to cytoskeletal dynamics during chemotaxis. *Dev. Cell* **9**, 19–34 (2005).
10. C. Janetopoulos, L. Ma, P. N. Devreotes, P. A. Iglesias, Chemoattractant-induced phosphatidylinositol 3,4,5-trisphosphate accumulation is spatially amplified and adapts, independent of the actin cytoskeleton. *Proc. Natl. Acad. Sci. U.S.A.* **101**, 8951–8956 (2004).
11. M. Postma, J. Roelofs, J. Goedhart, T. W. Gadella, A. J. Visser, P. J. Van Haastert, Uniform cAMP stimulation of *Dictyostelium* cells induces localized patches of signal transduction and pseudopodia. *Mol. Biol. Cell* **14**, 5019–5027 (2003).

12. M. Postma, J. Roelofs, J. Goedhart, H. M. Loovers, A. J. Visser, P. J. Van Haastert, Sensitization of *Dictyostelium* chemotaxis by phosphoinositide-3-kinase-mediated self-organizing signalling patches. *J. Cell Sci.* **117**, 2925–2935 (2004).
13. C. Arrieumerlou, T. Meyer, A local coupling model and compass parameter for eukaryotic chemotaxis. *Dev. Cell* **8**, 215–227 (2005).
14. M. Postma, P. J. Van Haastert, A diffusion-translocation model for gradient sensing by chemotactic cells. *Biophys. J.* **81**, 1314–1323 (2001).
15. A. Levchenko, P. A. Iglesias, Models of eukaryotic gradient sensing: Application to chemotaxis of amoebae and neutrophils. *Biophys. J.* **82**, 50–63 (2002).
16. B. Kutscher, P. Devreotes, P. A. Iglesias, Local excitation, global inhibition mechanism for gradient sensing: An interactive applet. *Sci. STKE* **2004**, pl3 (2004).
17. A. Gamba, A. de Candia, S. Di Talia, A. Coniglio, F. Bussolino, G. Serini, Diffusion-limited phase separation in eukaryotic chemotaxis. *Proc. Natl. Acad. Sci. U.S.A.* **102**, 16927–16932 (2005).

.